



## OPEN ACCESS

## EDITED BY

Zhaohui Zhang,  
Zhejiang University, China

## REVIEWED BY

Jhen-nien Chen,  
National Taiwan University, Taiwan  
Saulwood Lin,  
National Taiwan University, Taiwan

## \*CORRESPONDENCE

Eleni Rousselaki  
✉ erousel@hcmr.gr

RECEIVED 20 October 2025

REVISED 22 December 2025

ACCEPTED 23 December 2025

PUBLISHED 19 January 2026

## CITATION

Rousselaki E, Michalopoulos P, Pavlidou A, Hatzianestis I, Kaberi H, Iliakis S and Rousakis G (2026) Early and deep diagenetic imprint in surficial pore fluids from the Olimpi mud volcano field (Eastern Mediterranean). *Front. Mar. Sci.* 12:1728781. doi: 10.3389/fmars.2025.1728781

## COPYRIGHT

© 2026 Rousselaki, Michalopoulos, Pavlidou, Hatzianestis, Kaberi, Iliakis and Rousakis. This is an open-access article distributed under the terms of the [Creative Commons Attribution License \(CC BY\)](https://creativecommons.org/licenses/by/4.0/). The use, distribution or reproduction in other forums is permitted, provided the original author(s) and the copyright owner(s) are credited and that the original publication in this journal is cited, in accordance with accepted academic practice. No use, distribution or reproduction is permitted which does not comply with these terms.

# Early and deep diagenetic imprint in surficial pore fluids from the Olimpi mud volcano field (Eastern Mediterranean)

Eleni Rousselaki\*, Panagiotis Michalopoulos, Alexandra Pavlidou, Ioannis Hatzianestis, Helen Kaberi, Stelios Iliakis and Grigoris Rousakis

Hellenic Centre for Marine Research, Institute of Oceanography, Anavyssos, Greece

This study provides high-resolution pore-fluid profiles of surficial sediments (down to 40 cm) from four submarine mud volcanoes (MVs) of the Olimpi Mud Volcano Field (OMVF) in the Eastern Mediterranean, including the Gelendzhik, Heraklion, Moscow and Milano MVs. Here, we present major ions ( $\text{Na}^+$ ,  $\text{K}^+$ ,  $\text{Mg}^{2+}$ ,  $\text{SO}_4^{2-}$ ,  $\text{Cl}^-$ ), sulfide, methane, dissolved inorganic carbon (DIC),  $\delta^{13}\text{C}_{\text{DIC}}$ , ammonium, phosphate and silicate concentrations. These results were evaluated in relation to both early and deep diagenetic processes shaping pore-fluid chemistry. The four MVs can be classified into two geochemical groups: Gelendzhik and Heraklion, dominated by deep-sourced hypersaline fluids from Messinian salt dissolution and Moscow and Milano MVs, characterized by pore fluids largely reflecting seawater-derived compositions. In the hypersaline group, signatures of deep processes persist such as smectite–illite conversion at Heraklion and ammonium and methane upward migration, demonstrating that near-surface pore fluids retain the imprint of deep diagenesis. Organic matter oxidation via sulfate reduction (OSR) and anaerobic oxidation of methane coupled to sulfate reduction (AOM-SR) were also active, even within the hypersaline environments of the Gelendzhik and Heraklion MVs, as evidenced from stoichiometric ratios of  $\Delta\text{DIC}$  and  $\Delta\text{SO}_4^{2-}$  and  $\delta^{13}\text{C}_{\text{DIC}}$  isotopic data. In the hypersaline Gelendzhik MV, the diagenetically added DIC, representing the isotopic signature of mineralized organic matter, is estimated at  $-53.1\%$ , further indicating active AOM-SR under extreme salinity.

Overall, our findings demonstrate that deep-sourced fluids shape near-surface pore-fluid chemistry, generating pronounced heterogeneity among MVs and provide rare geochemical evidence of microbial resilience in hypersaline submarine environments.

## KEYWORDS

ammonium, anaerobic oxidation of methane, diagenesis, hypersaline fluid, mineral alteration, mud volcano, pore-water, sulfate reduction

## 1 Introduction

Mud volcanoes (MVs) serve as pathways for deep-seated fluids and gases to reach the seafloor (Milkov, 2000; Dimitrov, 2002; Mazzini and Etiope, 2017) and are clustered in areas of active plate boundaries (Kopf, 2002). There are more than 100 MVs in the Mediterranean Sea (Dimitrov, 2002; Kopf, 2002), influencing fluid migration, sediment degassing and biochemical cycling (Dimitrov, 2002; Ijiri et al., 2023).

Pore fluids composition in MVs reflects interacting deep and shallow processes, including sediment consolidation, mineral alteration (e.g., dehydration) and methane and carbon dioxide generation from organic matter decomposition (Moore and Vrolijk, 1992; Martin et al., 1996). All these processes modify fluids during ascent and near the sediment-water interface (Hensen et al., 2007). MV fluids expelled from depths of hundreds to thousands of meters below the seafloor (mbsf) undergo significant chemical and isotopic changes during diagenesis (Kastner et al., 1991; Martin et al., 1996). In addition, rapid shifts in response to tectonic processes such as arc rifting (Zhang, 2020), can result in fluid compositions that differ from seawater (Aloisi et al., 2004). Fluid flow varies spatially and temporally (Aloisi et al., 2004; Haese et al., 2006), with intense advection processes producing the largest deviations from seawater composition (Hensen et al., 2007). The deposition of a massive mud flow represents a major perturbation of surface sediments and associated pore waters, with fluid advection followed by molecular diffusion, which progressively shapes pore-fluid concentrations (Haese et al., 2006).

Despite extensive studies on pore-water geochemistry in MVs, most previous work has focused on deeper sediment layers (e.g. Dählmann and de Lange, 2003; Aloisi et al., 2004; Hensen et al., 2007; Vanneste et al., 2011; Zhang, 2020; Behrendt et al., 2023), while near-surface sediments have received relatively little attention (e.g. Aloisi et al., 2004; Haese et al., 2006). As a result, the influence of deep-sourced fluids on pore-water chemistry in the shallowest sediments, those directly interacting with the seafloor environment, remains poorly constrained.

The Olimpi Mud Volcano Field (OMVF) is located south of Crete and covers an area exceeding 6000 km<sup>2</sup>, representing the largest known mud volcano field along the Mediterranean Ridge (Huguen et al., 2005), which is associated to the collision between the African and Eurasian tectonic plates (Kopf et al., 2000). The seafloor structures of the OMVF are mainly related to backthrust faults (Behrendt et al., 2023). Previous pore-water studies at the OMVF have reported fluids enriched in ions such as Na<sup>+</sup> and Cl<sup>-</sup> and sulfate due to halite and gypsum dissolution, derived from Messinian salts (Böttcher et al., 1998; Dählmann and de Lange, 2003). The chemistry of seeping fluids in eastern Mediterranean cold seeps reflects spatial hydrological heterogeneity, suggesting that multiple fluid sources and discrete transport pathways may feed a single mud-volcano seep (Haese et al., 2006).

In this study, we employ a multidisciplinary approach to identify the dominant processes controlling fluid composition and to explain the spatial heterogeneity among four MVs within the

OMVF. To this end, we present high resolution profiles of pore fluids from surficial eruptive sediments from the Olimpi mud volcano field (OMVF), including concentrations of major ions (e.g., Na<sup>+</sup>, SO<sub>4</sub><sup>2-</sup>, Cl<sup>-</sup>), ammonium, phosphate, silicate, dissolved inorganic carbon (DIC),  $\delta^{13}\text{C}_{\text{DIC}}$ , sulfide, and methane. Our aim is to evaluate how deep-sourced fluids affect major ions concentrations through the dissolution of Messinian evaporites and the diagenesis of silicate minerals, spatial heterogeneity of ammonium due to inputs from deeper sediment layers, early diagenetic processes, potential for OSR and AOM under hypersaline conditions, as well as the imprint of deep sourced fluids on the DIC pool.

We investigate two contrasting geochemical groups within the OMVF, Gelendzhik and Heraklion, dominated by deep-sourced hypersaline fluids, and Moscow and Milano, characterized by pore water compositions largely reflecting seawater-derived signatures. By explicitly contrasting these two groups, this study provides a conceptual framework to understand solute and methane dynamics, and the interplay of deep and shallow diagenetic processes, in submarine mud volcano systems.

## 2 Study area and methods

### 2.1 Site background

The OMVF has been the focus of several investigations concerning mud volcanism, fluid seepage, and gas hydrates occurrence (e.g. Camerlenghi et al., 1992; Cita et al., 1996; Limonov et al., 1996). The geomorphology of the OMVF is characterized by important sub-circular features and high backscatter patches (Huguen et al., 2004). The MVs within the field display diverse geological morphologies: for example, the Milano MV is a well-defined circular dome, measuring up to 2 km in diameter (Huguen et al., 2004). The Moscow and Gelendzhik mud plateaus are asymmetric in cross section (Dimitrov, 2002; Huguen et al., 2004). Among the studied structures, the Gelendzhik MV is the largest and comprises a cluster of closely spaced MVs whose mud flows overlap (Limonov et al., 1996). The Heraklion MV, located ~ 15 km northwest of the main crater of the Gelendzhik plateau, has a ~3 km diameter sub-circular base (Panagiotopoulos et al., 2020).

The sampling sites (Table 1) were located on the crests of the Gelendzhik, Heraklion, Moscow, and Milano MVs (Figure 1). Gelendzhik, Moscow, and Milano MVs were selected because they are among the largest MVs in the OMVF, together with the newly discovered Heraklion MV during the LEVECO cruise.

### 2.2 Materials and methods

Sediment cores were collected in April 2016, during the LEVECO cruise, with the *R/V Aegaeo*. At each sampling site, a core was retrieved for pore-water extraction with the use of a multi corer (up to ~40 cm), where a high-resolution profile was obtained.

TABLE 1 Location, water column depth, sampling method, and core length of the sites sampled during the LEVECO cruise in April 2016.

Site	Latitude (°N)	Longitude (°E)	Depth (m)	Sampling method	Core length (cm)
Gelendzhik	33°54'1682	24°16'1408	1700	Multi corer	28
Heraklion	33°56'2670	24°06'8457	1722	Multi corer	34
Moscow	34°40'6178	24°31'5417	1833	Multi corer	30
Milano	34°43'9852	24°46'6365	1950	Multi corer	28

During sampling at the Gelendzhik MV, gas bubbles were observed emanating from the sediment. Notably, the core collected there was compressed from 28 to 18 cm due to degassing, whereas no significant compaction was recorded at the other sampling sites.

The sediment cores were immediately placed in a nitrogen-filled glove bag, prior to the removal of the remaining overlying water. The cores were sectioned at a resolution of 0.5 cm for the uppermost 2 cm, 1 cm from 2 to 10 cm depth, and 2 cm intervals below 10 cm.

Wet sediment samples were transferred into 50 mL plastic centrifuge tubes, which were then sealed, removed from the glove bag, and centrifuged at 4000 rpm for 20 minutes. Following centrifugation, the tubes were returned to the glove bag, and the supernatant was extracted using a 10 mL plastic syringe and passed through a 0.45 μm cellulose acetate filter for pore-water collection.

Subsamples were collected for dissolved nutrients (ammonium, phosphate, silicate), sulfide, DIC, δ<sup>13</sup>C<sub>DIC</sub> and major ions analyses

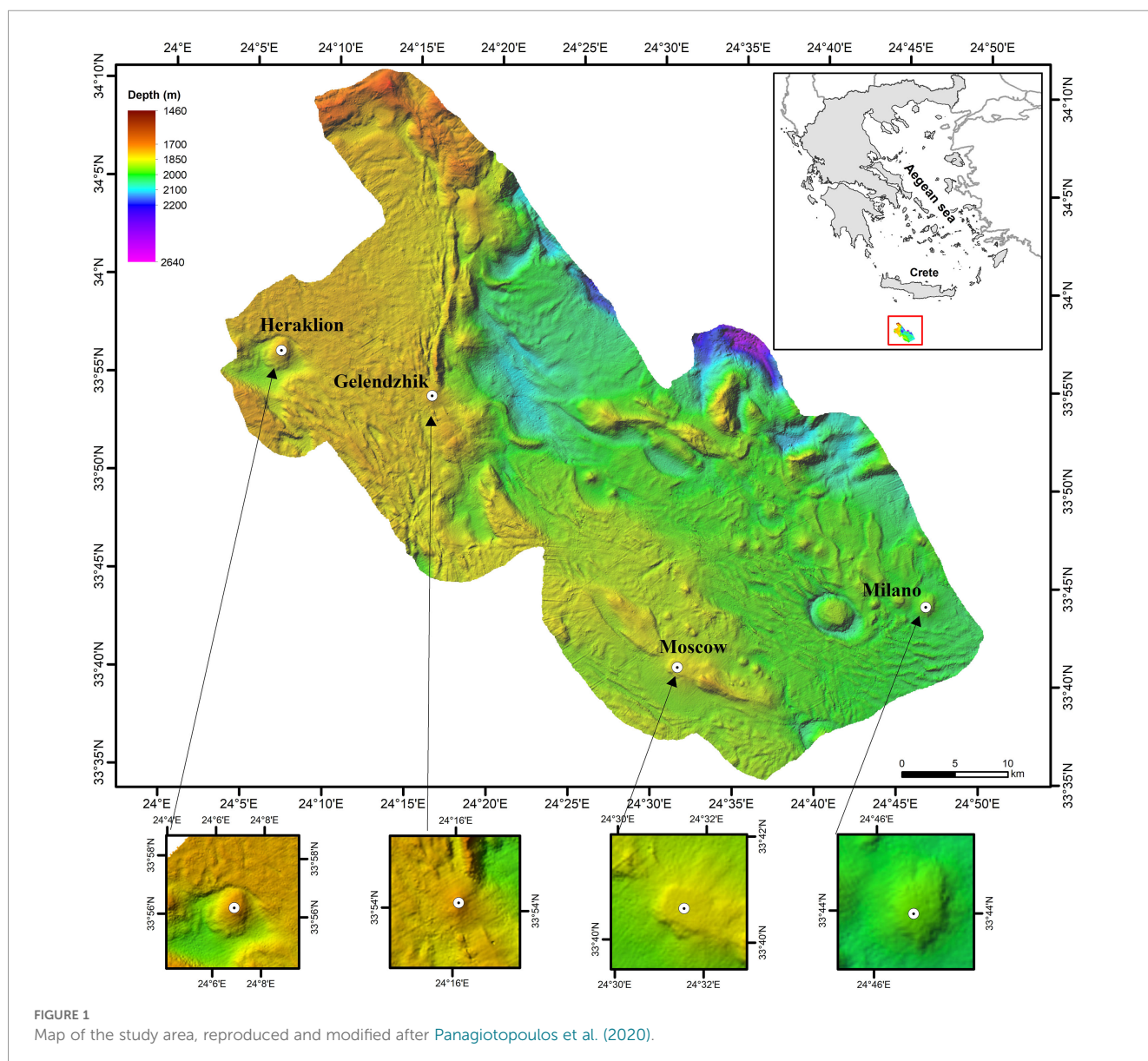


FIGURE 1 Map of the study area, reproduced and modified after Panagiotopoulos et al. (2020).

under a nitrogen atmosphere. Samples for nutrient analysis were stored at  $-20^{\circ}\text{C}$  until analysis. Ammonium was analyzed using a Perkin Elmer Lambda 25 spectrophotometer following appropriate dilution, according to the method of [Koroleff \(1970\)](#). Phosphate and silicate concentrations were determined with a SEAL AutoAnalyzer AA3, following the protocols of [Murphy and Riley \(1962\)](#) and [Mullin and Riley \(1955\)](#), respectively. Sulfide was analyzed spectrophotometrically on board immediately after sampling, using the method of [Cline \(1969\)](#). The measurement represents the sum of  $\text{H}_2\text{S}$ ,  $\text{HS}^-$ , and  $\text{S}^{2-}$  concentrations, hereinafter referred to as sulfide. Samples for DIC analysis were preserved with saturated mercuric chloride solution and analyzed by flow injection analysis ([Hall and Aller, 1992](#)). Samples for  $\delta^{13}\text{C}_{\text{DIC}}$  analysis were stored frozen in vials sealed with septa and aluminum caps ([Bryant et al., 2013](#)). Data are reported in standard  $\delta$ -notation as ‰ relative to the VPDB standard. Pore-water samples for major anion analysis were stored at  $4^{\circ}\text{C}$ . Major ions were analyzed by Metrohm ion chromatography following appropriate dilution. Concentrations of sulfate, calcium, and magnesium were corrected based on reference values obtained from a certified seawater standard. Methane samples were collected from pre-drilled tubes of the same multi-corer cast using 2 mL plastic cut-off syringes. The sample material was injected into 20 mL headspace vials, which were sealed with septa and aluminum caps, then baked at  $60^{\circ}\text{C}$  for 20 minutes ([Niewöhner et al., 1998](#)). Onboard methane analysis was performed by injecting 250  $\mu\text{L}$  of the vial headspace into a gas chromatograph equipped with an FID (Shimadzu 2010). Sediment samples were analyzed for organic carbon content and carbon isotopic composition at the ISO-Analytical laboratory. Data are reported in standard  $\delta$ -notation as ‰ relative to the VPDB standard.

## 3 Results

### 3.1 MVs with hypersaline dominated fluids (Gelendzhik and Heraklion)

The profiles of major ions ( $\text{Cl}^-$ ,  $\text{Na}^+$ ,  $\text{K}^+$ ,  $\text{SO}_4^{2-}$ ,  $\text{Ca}^{2+}$ ,  $\text{Mg}^{2+}$ ) revealed elevated concentrations at Gelendzhik and Heraklion ([Figure 2](#)). Maximum  $\text{Na}^+$  and  $\text{Cl}^-$  values reached 2116 and 1989 mM at Gelendzhik, and 3189 and 2392 mM at Heraklion, well above seawater ( $\sim 513$  mM  $\text{Na}^+$  and  $\sim 598$  mM  $\text{Cl}^-$ ).  $\text{K}^+$  concentrations increased downcore at Gelendzhik, closely following  $\text{Na}^+$  and  $\text{Cl}^-$  trends, while a slight downcore decrease was observed at Heraklion. Sulfate also increased with depth, reaching  $\sim 166$  mM at Gelendzhik and 51 mM at Heraklion.  $\text{Ca}^{2+}$  and  $\text{Mg}^{2+}$  displayed downcore increases at Gelendzhik, whereas at Heraklion decreased downcore.  $\text{Na}^+/\text{Cl}^-$  ratios were elevated (up to 1.06 at Gelendzhik and 1.33 at Heraklion), and the sulfate-to-chloride ratio was notably high at Gelendzhik (0.083) and 0.021 at Heraklion. Most of the solute profiles at the Gelendzhik ( $\text{Na}^+$ ,  $\text{Cl}^-$ ,  $\text{K}^+$ ,  $\text{Mg}^{2+}$  and sulfate) and Heraklion ( $\text{Na}^+$ ,  $\text{Cl}^-$ ,  $\text{K}^+$ ,  $\text{Mg}^{2+}$ ,  $\text{Ca}^{2+}$  and sulfate) sites show that, following fluid deposition, diffusion dominates and the profiles do not appear to have reached steady

state. The deeper part of  $\text{Ca}^{2+}$  profile, at Gelendzhik, appears to be alteration-dominated.

Sulfide concentrations were high near the sediment–water interface at Gelendzhik, reaching  $1235\ \mu\text{M}$  at 8–12 cmbsf, while at Heraklion, maximum sulfide occurred deeper, at 22–24 cmbsf, reaching  $1519\ \mu\text{M}$  ([Figure 3](#)). Methane concentrations increased downcore at both sites, with a strikingly high value of  $24,834\ \mu\text{M}$  at 26 cmbsf at Gelendzhik, and  $2707\ \mu\text{M}$  at the bottom of Heraklion cores. DIC concentrations increased with depth, and  $\delta^{13}\text{C}_{\text{DIC}}$  profiles showed progressive downcore depletion at Heraklion, while Gelendzhik exhibited a more complex pattern with initial depletion near the sediment surface ( $-10.2\%$ ) followed by a further downcore decrease ( $-22.4\%$  at  $\sim 14$  cmbsf), and then a subsequent enrichment ( $-16.1\%$  at  $\sim 18$  cmbsf).

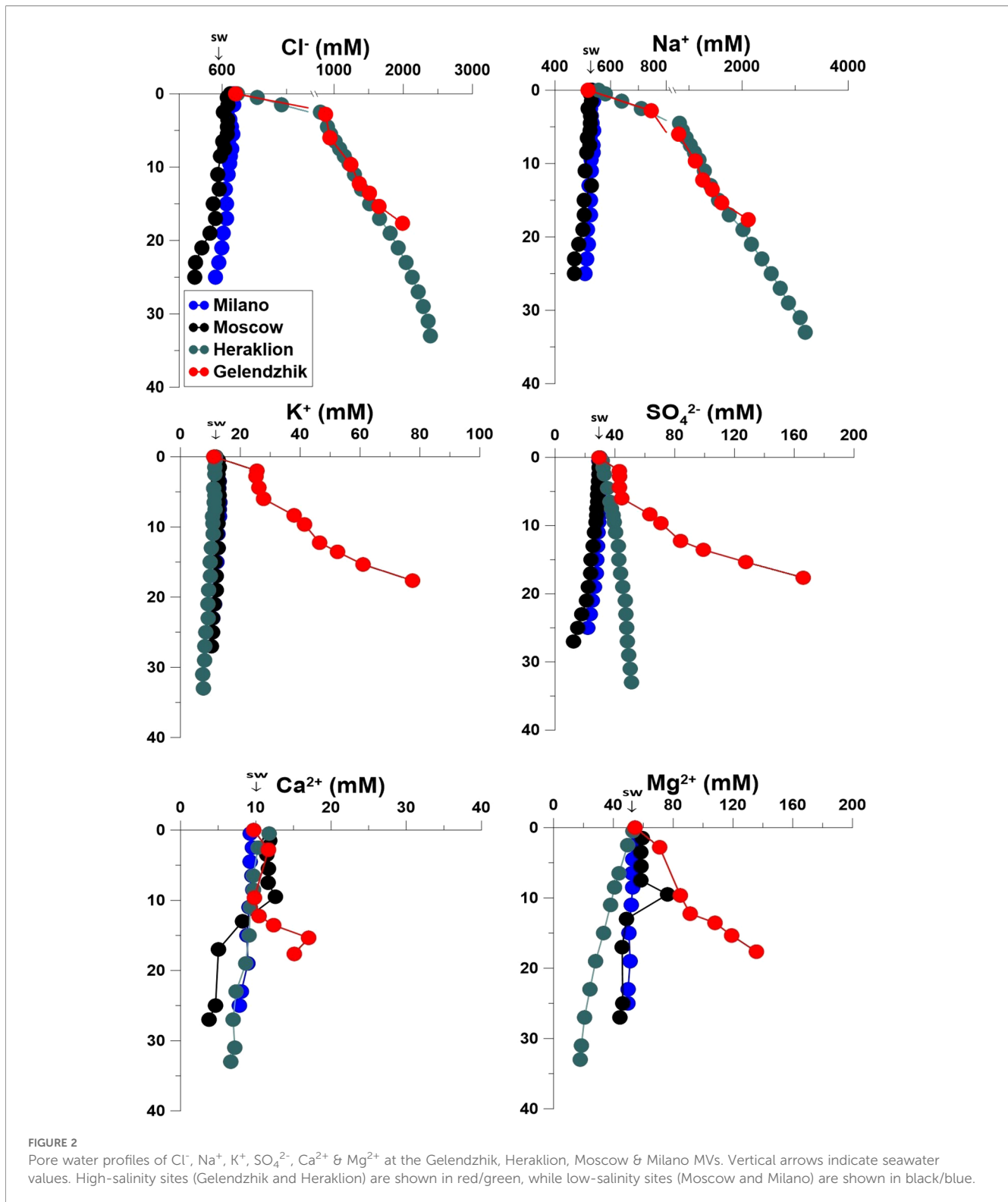
Ammonium concentrations increased with depth, peaking at  $7235\ \mu\text{M}$  at Gelendzhik and  $1273\ \mu\text{M}$  at Heraklion. Phosphate concentrations were higher at Gelendzhik (up to  $17.1\ \mu\text{M}$ ) and relatively low at Heraklion (up to  $4.7\ \mu\text{M}$ ), with discrete subsurface maxima at 10 cmbsf. Silicate reached maximum values at Gelendzhik ( $\sim 229\ \mu\text{M}$ ). Ammonium-to-phosphate ratios were up to 1182 at Gelendzhik and 424 at Heraklion, while ammonium-to-DIC ratios were up to 1.05 and 0.33, respectively ([Figure 4](#)).

### 3.2 MVs with near-seawater dominated fluids (Moscow and Milano MVs)

At the Moscow and Milano MVs,  $\text{Na}^+$  and  $\text{Cl}^-$  concentrations were closer to seawater values, with slight downcore decreases ( $536$  &  $584$  mM, respectively), and  $\text{K}^+$ ,  $\text{Ca}^{2+}$ , and  $\text{Mg}^{2+}$  generally decreased with depth ([Figure 2](#)), suggesting removal processes affecting these cations such as carbonate or other mineral precipitation ([Martin et al., 1996](#)), or may also reflect mixing with deeper fluids depleted in these cations ([Hensen et al., 2007](#)).  $\text{Na}^+/\text{Cl}^-$  ratios were near that of seawater 0.86 (0.87–0.88), and sulfate-to-chloride ratios remained below that of seawater 0.051 ( $-0.021$ – $0.037$ ) ([Figure 5](#)). The solute profiles at the Milano and Moscow sites are not concave, indicating diffusion-dominated behavior, particularly in the upper sections of the studied cores (up to 10 cmbsf).

Sulfide concentrations fluctuated less at these sites and were absent in the uppermost 4 cmbsf at Moscow and 8 cmbsf at Milano. Methane increased downcore, reaching  $255\ \mu\text{M}$  at Moscow and  $2026\ \mu\text{M}$  at Milano. DIC generally increased with depth, with the highest value of  $15.5$  mM at Milano.  $\delta^{13}\text{C}_{\text{DIC}}$  profiles showed surface values near  $0\%$ , becoming progressively more negative downcore, reaching  $-17.3\%$  at Moscow and  $-29.6\%$  at Milano ([Figure 3](#)).

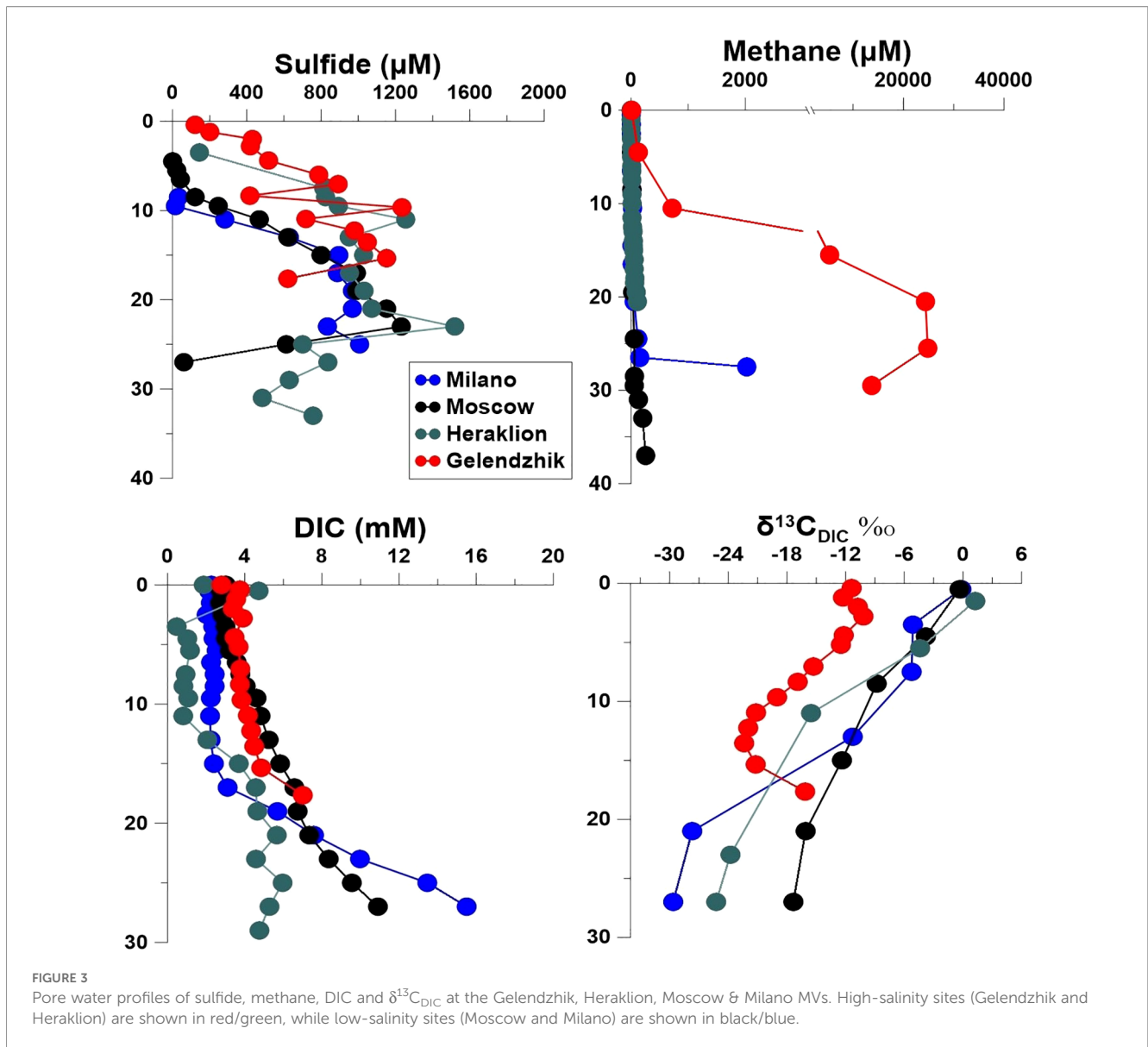
Ammonium increased with depth, but maximum values were lower than at high-salinity MVs ( $84\ \mu\text{M}$  at Moscow,  $130\ \mu\text{M}$  Milano). Phosphate concentrations remained relatively low (up to  $4.7\ \mu\text{M}$ ), with minor subsurface maxima at 18 cmbsf at Moscow MV and 20 cmbsf at Milano. Silicate concentrations were generally lower than at Gelendzhik ( $128$  and  $144\ \mu\text{M}$  at Moscow and Milano MVs). Ammonium-to-phosphate and ammonium-to-DIC ratios were also markedly lower ([Figure 4](#)).



### 3.3 Sediment organic carbon and $\delta^{13}\text{C}_{\text{org}}$

Figure 6 presents the vertical profiles of organic carbon content ( $C_{\text{org}}$ ) and  $\delta^{13}\text{C}_{\text{org}}$  in sediment samples from the Gelendzhik, Moscow and Heraklion MVs. At Moscow MV,  $C_{\text{org}}$  content remained relatively stable, while  $\delta^{13}\text{C}_{\text{org}}$  values ranged from

-26.1‰ to -23.8‰. At the Heraklion MVs, the highest organic carbon content values are found within the upper ~0–10 cmbsf interval, with the maximum value of 2.17% measured at 1.5 cmbsf. This zone also coincides with more negative  $\delta^{13}\text{C}_{\text{org}}$  values (Figure 6). The most depleted  $\delta^{13}\text{C}_{\text{org}}$  values measured were -26.8‰ at Gelendzhik and -28.6‰ at Heraklion (Figure 6). This



could suggest the presence of methane related biomass (Haese et al., 2003). At the sulfate depletion zone, AOM-specific biomarkers are enriched, which is associated with pronounced  $^{13}\text{C}$  depletion in bulk organic carbon (Haese et al., 2003).

## 4 Discussion

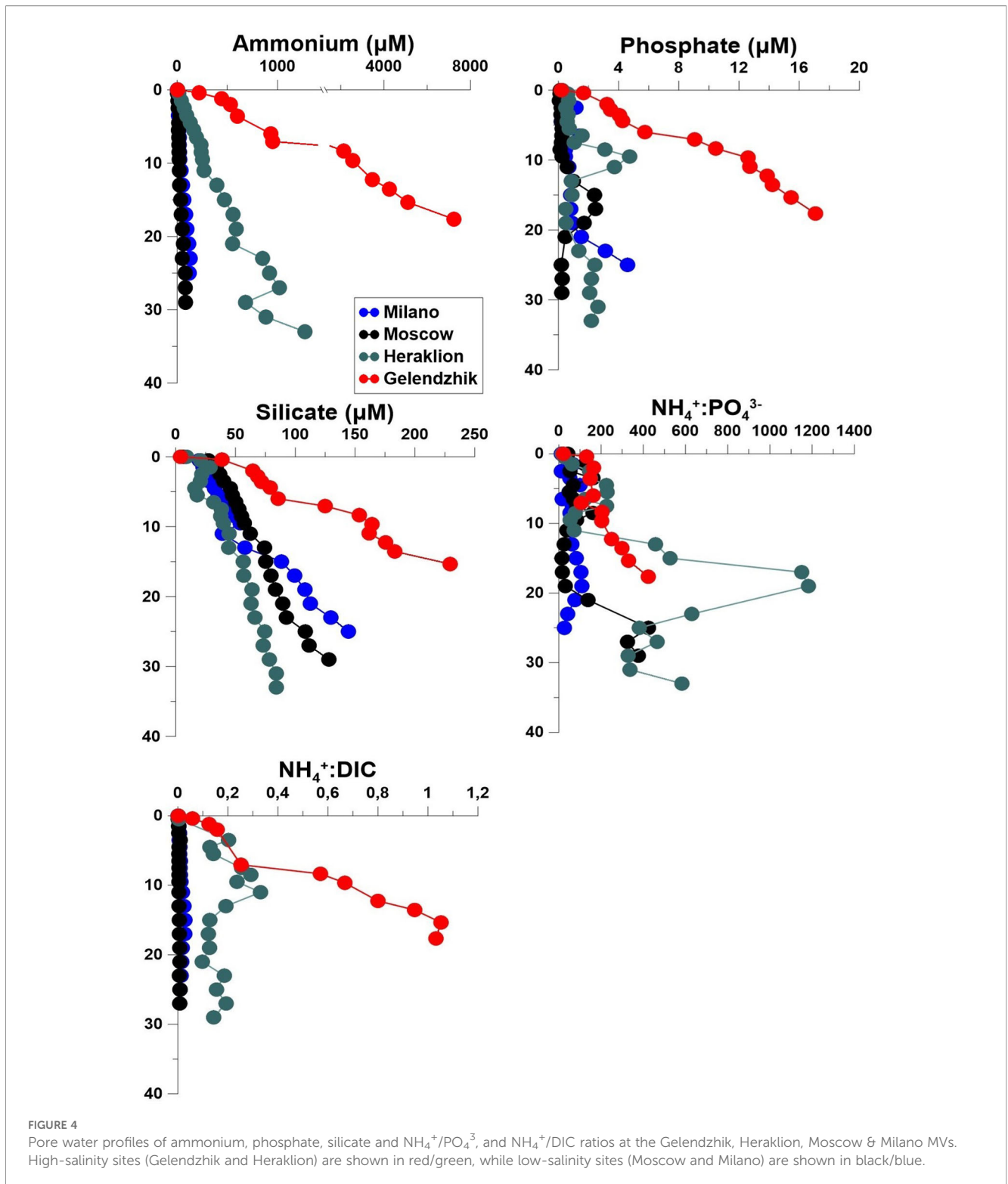
The Moscow and Milano MVs form a group with ion concentrations near those of seawater. In contrast, the Gelendzhik and Heraklion MVs are enriched in chloride, sodium, and sulfate, with concentrations well above seawater values, forming a hypersaline environment near the sediment–water interface. We examine the factors contributing to the spatial heterogeneity of the surficial pore fluids among the studied MVs in the OMVE, with a particular effort to distinguish the deep-sourced diagenetic imprint on pore-fluid composition.

### 4.1 Deep-sourced fluid signatures controlled by Messinian evaporite dissolution and diagenetic reactions

#### 4.1.1 Halite and gypsum derived imprint in $\text{Na}^+$ , $\text{Cl}^-$ , $\text{SO}_4^{2-}$ at the Gelendzhik and Heraklion MV

Chloride behaves conservatively during most diagenetic processes, making it a useful tracer for identifying the mixing of fluids from different sources (Martin et al., 1996). In contrast, many others solutes are directly altered by diagenetic reactions, thereby changing solute-to-chloride ratios (Martin et al., 1996). Consequently, chlorinity anomalies and solute-versus-Cl profiles are commonly used to distinguish between fluid sources and diagenetic alterations (Martin et al., 1996).

The  $\text{Na}^+$  and  $\text{Cl}^-$  profiles at the Gelendzhik and Heraklion MVs are curved upwards (Figure 2), indicative of upward fluid advection (Bohrmann et al., 2003; Aloisi et al., 2004). Either way, their

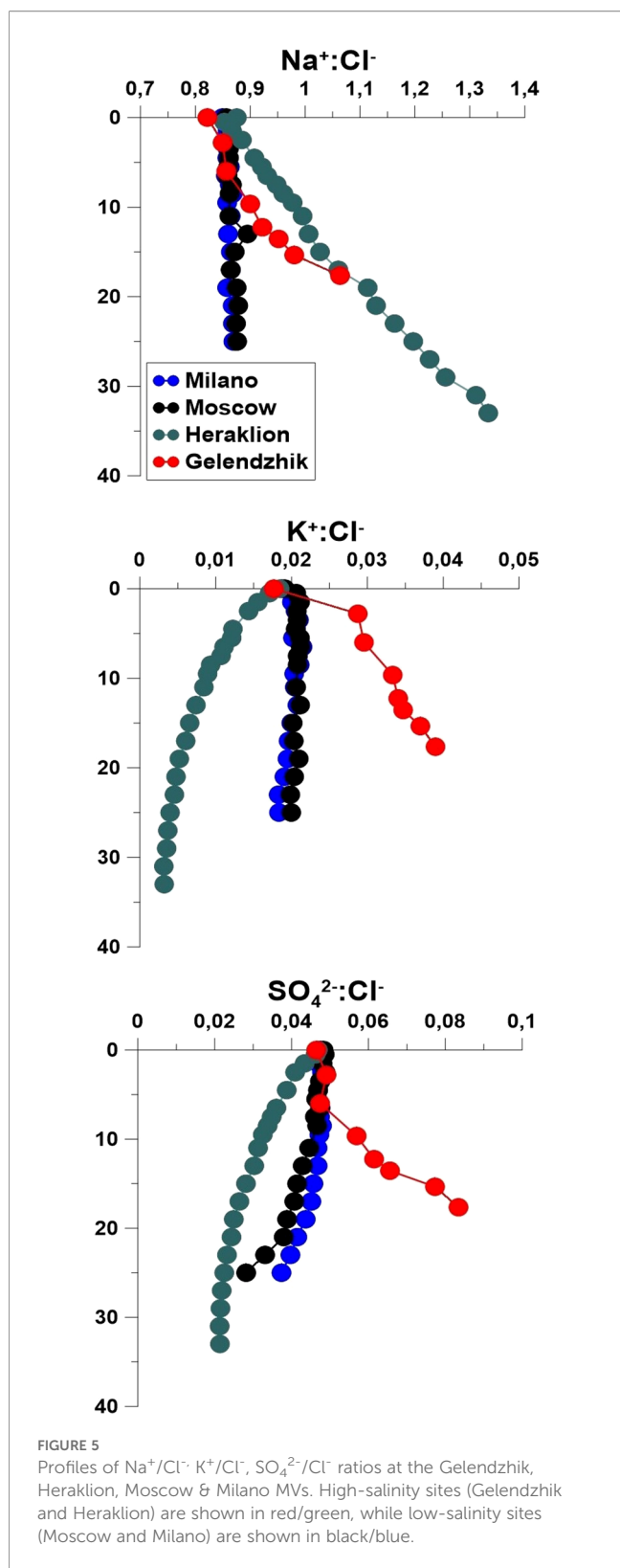


chemical imprint indicates upward migration of evaporite-derived fluids. Chlorinity in deeper fluids is approximately 3–4 times higher than that of seawater (Figure 2), consistent with values previously reported at the OMVF (e.g. Haese et al., 2006; Behrendt et al., 2023).

At the Gelendzhik MV, the  $\text{Na}^+/\text{Cl}^-$  ratios range between 0.85 and 1.06 (Figure 5) and  $\text{Cl}^-$  and  $\text{Na}^+$  show a strong correlation (0.995),

suggesting addition of both ions through halite dissolution (Aloisi et al., 2004) within the Messinian salts (Dählmann and de Lange, 2003). Similarly, at the Heraklion MV,  $\text{Na}^+$  and  $\text{Cl}^-$  are strongly correlated (0.993, see Supplementary material\_Table S2) indicating a similar source.

Sulfate concentrations at both sites exceed the seawater value and correlate significantly with  $\text{Na}^+$  and  $\text{Cl}^-$  (both  $r > 0.98$ ,  $p < 0.01$ )



supporting an evaporitic origin. Sulfate enrichment in the OMVF has been attributed to gypsum dissolution (Böttcher et al., 1998; Omeregje et al., 2009), with  $\delta^{34}\text{S}$  and  $\delta^{18}\text{O}$  signatures further pointing to a Messinian evaporitic source (Böttcher et al., 1998).

#### 4.1.2 Contrasting K<sup>+</sup>, Ca<sup>2+</sup> and Mg<sup>2+</sup> behavior at the Gelendzhik and Heraklion MV

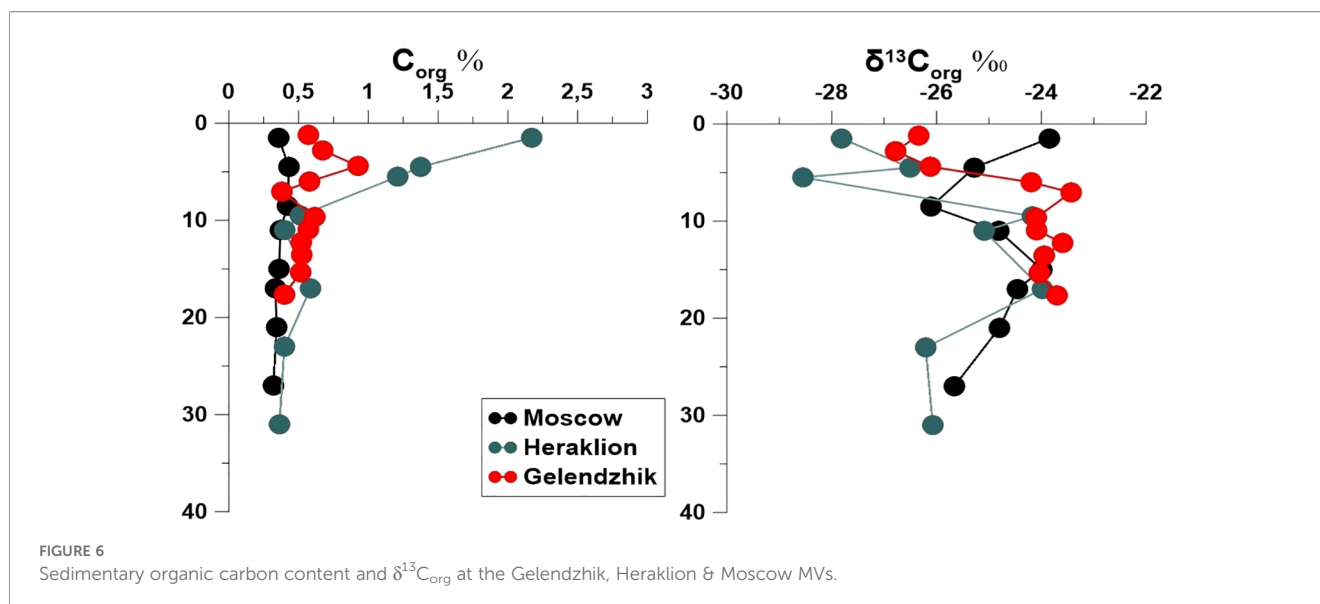
Although Messinian salts dissolution is evident at both Gelendzhik and Heraklion MV, K<sup>+</sup> and Mg<sup>2+</sup> concentrations indicate different diagenetic processes. At the Gelendzhik MV, high Ca<sup>2+</sup> and Mg<sup>2+</sup> concentrations likely reflect carbonate or gypsum dissolution, whereas strong enrichment of K<sup>+</sup> (up to eight times seawater value, Figure 2) suggests involvement of a different mineral reaction. One possibility is that fluids originated from salt differing from those at other MVs, K and Mg enrichment has been attributed to mixing with fluids sourced from evaporites other than Mg-rich salts (e.g. bischofite) (Behrendt et al., 2023). Alternatively, subsurface silicate weathering could account for the release of bicarbonate along with Ca<sup>2+</sup>, Mg<sup>2+</sup>, Na<sup>+</sup>, and K<sup>+</sup> into the pore fluids (Wallmann et al., 2008; Scholz et al., 2013). This interpretation is supported by the strong positive correlation between K<sup>+</sup> and silicate ( $r = 0.937$ ), and the higher silicate concentrations at this site. While silicate weathering should increase DIC, no pronounced DIC enrichment is observed (Figure 3). However, DIC production during silicate weathering may be counterbalanced by consumption during methanogenesis, potentially masking the weathering signal, as silicate weathering can buffer a substantial fraction of CO<sub>2</sub> produced by methanogenesis (Torres et al., 2020).

In contrast, fluids at the Heraklion MV display Na/Cl ratios between 0.85 and 1.26 (Figure 5), with values exceeding unity in deeper samples, indicating excess Na<sup>+</sup>. Such high Na/Cl ratios have also been reported in other mud volcanoes fields (Li et al., 2014). Elevated Na/Cl ratios, together with downcore K<sup>+</sup> depletion (K/Cl < 0.01 below 10 cmbsf) and significant negative correlations between K<sup>+</sup> and Na<sup>+</sup>, Cl<sup>-</sup>, SO<sub>4</sub><sup>2-</sup>, and silicate (see Supplementary material Table S2), point to smectite-illite transformation prior to fluid ascent (Martin et al., 1996; Hensen et al., 2007). This reaction involves uptake of K<sup>+</sup> and release of Na<sup>+</sup>, leading to relative Na enrichment and K depletion compared to seawater.

Fluid compositions at both MVs indicate mobilization from a deep source layer beneath the Messinian salts, producing hypersaline ascending fluids. At Gelendzhik, Mg-K enrichments indicate a deep evaporite-derived fluid modified during ascent either through mixing with K-rich salts or through water-rock interaction with silicate minerals. At Heraklion illitization has led to K<sup>+</sup> depletion and Na<sup>+</sup> enrichment. This interpretation aligns with previous studies suggesting that the highly saline fluids point to the same endmember across the OMVF (Behrendt et al., 2023) which undergoes various alteration processes during ascension, influencing their final fluid signatures.

#### 4.1.3 Depth of fluid origin at Heraklion MV

Heraklion is the only site where smectite-to-illite transformation is evident, even in shallow pore fluids. This reaction begins at approximately 60 °C and is nearly complete by around 160 °C (Kastner et al., 1991). Assuming a geothermal gradient of 30–35 °C/km for the Olimpi field (Camerlenghi et al., 1995), these temperatures correspond to fluid mobilization depths



of ~2 to 5 km, supporting a deep-seated fluid source. It is also worth noting that, the mud flows indentified during the LEVECO cruise, were inferred to originate from sediments no deeper than approximately 2 kmbsf (Panagiotopoulos et al., 2020). This points to a decoupling between sediment and fluid mobilization depth, in agreement with previous studies in the OMVF (Deyhle and Kopf, 2001) and other mud volcano systems (Li et al., 2014; Doll et al., 2023).

#### 4.1.4 Moscow and Milano: the low salinity sites

At the Moscow and Milano MVs, Na/Cl and K/Cl ratios remain close to seawater values (Figure 5). However, both  $\text{Cl}^-$  and  $\text{Na}^+$  concentrations decrease with depth, indicating mild pore-water freshening.  $\text{Cl}^-$  concentrations decrease to 536 mM and 584 mM at Moscow and Milano, respectively, compared to near-surface values 619 mM and 627 mM. Similarly,  $\text{Na}^+$  concentrations decrease from 530 mM and 533 mM at the surface to 470 mM and 508 mM at depth.

Clay minerals dehydration, particularly smectite-to-illite transformation is considered the most significant dehydration process in marine forearc environments (Saffer and Tobin, 2011) and has been identified as a key control on pore water isotopic composition (Dählmann and de Lange, 2003). The observed chlorinity decrease may therefore reflect smectite-to-illite transformation occurring at depth, prior to fluid ascent near the surface. However, the absence of  $\text{K}^+$  depletion and  $\text{Na}^+$  enrichment relative to  $\text{Cl}^-$  prevents a conclusive attribution of the freshening to this process.

Our results highlight pronounced spatial variability in pore fluid concentrations across the studied MVs. Previous work has shown that substantial heterogeneity can also occur within individual MVs, such as the Carlos Ribeiro MV (Vanneste et al., 2011) and the Milano MV (Haese et al., 2006). At Milano, both saline-enriched and freshened fluids were reported within a

distance of only ~500 m, suggesting that single mud volcanoes may be fed by multiple fluid sources (Haese et al., 2006).

#### 4.2 Ammonium enrichment in the hypersaline fluids at Gelendzhik and Heraklion MVs

Pore fluid ammonium concentrations show a clear contrast between the two geochemical groups in this study. The pore fluid chemistry at Gelendzhik and Heraklion MV is characterized by elevated ammonium concentrations, reaching up to 7235  $\mu\text{M}$  and 1273  $\mu\text{M}$ . In contrast the highest ammonium concentrations at the Moscow and Milano MVs were much lower, 80  $\mu\text{M}$  and 130  $\mu\text{M}$  (Figure 4). This spatial variability indicates distinct sources.

The high ammonium concentrations observed at Gelendzhik and Heraklion are unlikely to have been produced within the surficial sediments, given their relatively low organic carbon sediment content (Figure 6), which reaches only 0.40% at Gelendzhik and 0.36% at Heraklion in the deepest samples. Notably, similarly low sedimentary organic carbon contents are observed at Moscow MV (0.43%), yet ammonium concentrations remain much lower, excluding *in situ* organic matter degradation as the dominant ammonium source.

At Gelendzhik and Heraklion, ammonium displays strong positive correlations ( $p < 0.01$ ) with chloride and sulfate ( $r = 0.993$ – $0.959$  and  $0.993$ – $0.908$ , respectively), indicating a common source and co-mobilization during upward fluid transport. Such correlations point to ammonium release from deeper zones, consistent with previous observations of ammonium-rich fluids ( $>1000 \mu\text{mol/L}$ ) derived from the deeper strata (Masuzawa et al., 1992; Bohrmann et al., 2003; Aloisi et al., 2004).

To further investigate ammonium sources, we examined its relationship with phosphate and DIC.  $\text{NH}_4^+:\text{PO}_4^{3-}$  ratios at the

Gelendzhik and Heraklion MVs exceed the Redfield ratio of 16:1, reaching values up to 424 and 1181, respectively (Figure 4). These elevated ratios suggest efficient phosphate removal along the fluid flow path, potentially through precipitation of phosphate-bearing minerals such as vivianite or carbonate fluorapatite below the sulfate–methane transition zone (Dijkstra et al., 2014; Egger et al., 2015), as previously reported in other mud volcanoes systems (López-Rodríguez et al., 2019).

$\text{NH}_4^+:\text{DIC}$  ratios further distinguish the two sites within the hypersaline setting. At Heraklion, ratios (0.15–0.19; Figure 4) are consistent with ammonium release during organic matter degradation following Redfield stoichiometry. In contrast, much higher  $\text{NH}_4^+:\text{DIC}$  ratios at Gelendzhik (0.95–1.05) indicate excess nitrogen relative to carbon. This excess may result from a combination of carbonate precipitation along the fluid flow path and DIC depletion associated with methane generation via pyrolysis of organic matter, which often leads to low carbon dioxide concentrations (Snyder et al., 2007). During methanogenesis, the ammonium-to-DIC release is approximately 0.30 (Wallmann et al., 2008), yet the  $\text{NH}_4^+:\text{DIC}$  ratios at Gelendzhik are even higher, suggesting additional carbon removal. These findings are consistent with the observed variability in methane concentrations, which are higher at Gelendzhik MV (Figure 3).

The elevated ammonium concentrations at Gelendzhik and Heraklion MVs are not derived from *in situ* organic matter decomposition, but from a deeper source, associated with upward fluid advection. In contrast the lack of ammonium enrichment at Moscow and Milano highlights the importance of the geological settings in controlling pore fluid chemistry across the studied MVs.

### 4.3 Sulfate reduction and anaerobic oxidation of methane

Sulfate reduction (SR) is a key terminal step in the mineralization of organic matter under anoxic conditions in marine sediments (Jørgensen et al., 2019b), accounting for approximately 25–50% of total organic carbon mineralization in ocean margin sediments (Jørgensen and Kasten, 2006). In methane-rich sediments, the anaerobic oxidation of methane (AOM) occurs by microbial consortia of archaea and sulfate-reducing bacteria (Hinrichs et al., 1999; Boetius et al., 2000), limiting methane emissions from marine sediments (Egger et al., 2016). In the absence of advective flow or gas bubble transport, AOM effectively limits upward methane diffusion before it reaches the overlying water (Jørgensen et al., 2019a).

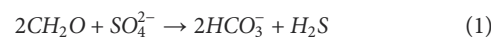
In this section, we use stoichiometric ratios and isotopic data to assess whether sulfate consumption at the studied MVs is dominated by organic matter oxidation linked to sulfate reduction (OSR) or anaerobic oxidation of methane coupled with sulfate reduction (AOM-SR).

#### 4.3.1 Stoichiometric ratios for sulfate consuming processes

At Moscow and Milano MVs, the  $\text{SO}_4:\text{Cl}$  ratios are consistently lower than those of Eastern Mediterranean seawater (~0.051)

(Thompson et al., 1931), except at the Gelendzhik MV (Figure 5). OSR and AOM-SR both consume sulfate and produce DIC, but with distinct stoichiometric relationships (Masuzawa et al., 1992; Kastner et al., 2008).

Organic matter oxidation linked to sulfate (OSR) can be described by Equation 1 (Masuzawa et al., 1992):



If  $\text{CH}_4$  is present in sufficient concentrations, AOM-SR may become the dominant process for  $\text{SO}_4^{2-}$  depletion in the pore water (Hensen et al., 2003), with higher activity under increased methane fluxes (Lee et al., 2021). AOM-SR can be described by Equation 2 (Boetius et al., 2000):



To distinguish between these pathways, we calculated the  $\Delta[\text{DIC} + \text{Ca}^{2+} + \text{Mg}^{2+}]$  and  $\Delta\text{SO}_4$ , where  $\Delta$  represents the concentration difference between the overlying water and the pore water at a given depth (Masuzawa et al., 1992; Kastner et al., 2008). Correction for  $\text{Ca}^{2+}$  and  $\text{Mg}^{2+}$  accounts for carbonate precipitation effects (Masuzawa et al., 1992; Kastner et al., 2008). A 1:1 slope in this plot indicates that AOM-SR is the dominant sulfate-consuming process. A slope between 1 and 2 suggests that both SR pathways are occurring simultaneously, while a slope 1:2 indicates OSR (Masuzawa et al., 1992; Kastner et al., 2008).

At the Gelendzhik MV, nearly all data points fall below the 1:1 slope, with an estimated slope of approximately 0.63 (Figure 7). Although lower than the theoretical AOM-SR ratio, this likely reflects DIC-depleted fluids and/or DIC loss due to methane degassing during core recovery (Haese et al., 2003), consistent with AOM-SR dominance. At the Heraklion MV, most data points fall between the 1:1 and 2:1 slope, implying that both OSR and AOM-SR co-occur (Figure 7). At the Milano MV, OSR appears to be the dominant process for sulfate consumption, as data points fall at the 2:1 slope (Figure 7). At the Moscow MV, OSR also appears to dominate. However, several data points lie well above the 2:1 slope, indicating excess DIC. This excess is likely attributed to diffusion of DIC from deeper zones (Kim et al., 2011), consistent with evidence of fluid flow at Moscow MV based on radio-tracing methods (Tsabaris et al., 2020).

#### 4.3.2 Isotopic evidence for sulfate-consuming processes

Stable carbon isotopes of DIC ( $\delta^{13}\text{C}_{\text{DIC}}$ ) provide additional insights on sulfate-consuming processes and carbon cycling.  $\delta^{13}\text{C}_{\text{DIC}}$  represents mixing between multiple carbon sources, including bottom water DIC, DIC carried by ascending fluids, DIC produced through methane oxidation, and DIC produced via organic matter oxidation (Lichtschlag et al., 2010). Consequently,  $\delta^{13}\text{C}_{\text{DIC}}$  values depend on the relative abundance of these sources (Aloisi et al., 2000). If OSR is the sole process involved,  $\delta^{13}\text{C}_{\text{DIC}}$  values are expected to range between that of bottom water (~0‰) and that of sedimentary organic carbon. In this study,  $\delta^{13}\text{C}_{\text{org}}$  values ranged between -23.4‰ to -28.6‰ (Figure 6), indicating a mixture of pelagic

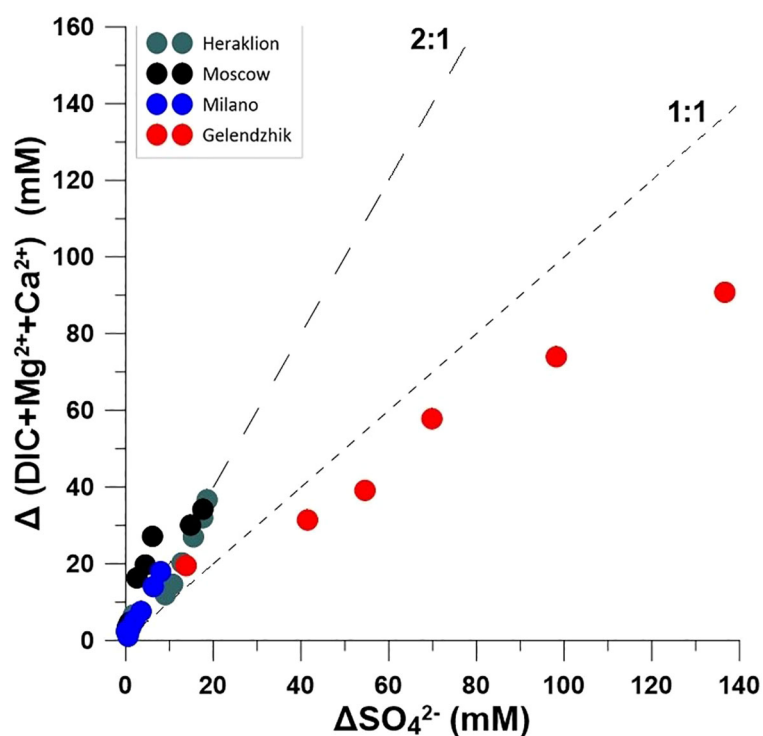


FIGURE 7

Plots of  $\Delta(\text{DIC}+\text{Mg}^{2+}+\text{Ca}^{2+})$  versus  $\Delta(\text{SO}_4^{2-})$  at the Gelendzhik, Heraklion, Moscow & Milano MVs.  $\Delta$  denotes the absolute difference in pore water concentrations between bottom-water and pore-water values at a given sampling depth.  $\Delta\text{Ca}$  and  $\Delta\text{Mg}$  are added to  $\Delta\text{DIC}$  to account for carbonate precipitation. A slope of 1:1 indicates sulfate reduction related to the anaerobic oxidation of methane (AOM-SR), while a 2:1 slope reflects sulfate reduction due to organic matter degradation (OSR).

organic matter ( $\sim -21\%$  in Eastern Mediterranean pelagic sediments (Fontugne and Calvert, 1992) and a more  $^{13}\text{C}$ -depleted fraction.

At the Milano MV,  $\delta^{13}\text{C}_{\text{DIC}}$  values showed a clear downcore decrease, reaching  $-29.6\%$  (Figure 3).  $\delta^{13}\text{C}_{\text{DIC}}$  values lower than those of typical organic matter ( $\sim -21\%$ ) indicate a significant contribution from anaerobic oxidation of methane (Chen et al., 2022). AOM-SR is typically associated with  $\delta^{13}\text{C}_{\text{DIC}}$  decrease toward the SMTZ (Kim et al., 2011), as methane-derived carbon is markedly in  $^{13}\text{C}$ -depleted (Borowski et al., 1996; Whiticar, 1999). At the Heraklion MV,  $\delta^{13}\text{C}_{\text{DIC}}$  values also decrease downcore to  $\sim -25.2\%$  (Figure 3), suggesting OSR dominance with a secondary contribution from AOM-SR, consistent with moderate methane concentrations and the stoichiometric ratios. In contrast, pore fluids at the Moscow MV exhibit less negative  $\delta^{13}\text{C}_{\text{DIC}}$  values, with a minimum of  $17\%$  at 26–28 cmbsf (Figure 3). Such values are consistent with a mixed DIC pool of OSR-derived DIC and upwardly diffusing DIC from deeper zones, where microbial reduction of  $\text{CO}_2$  to  $\text{CH}_4$  preferentially removes the lighter  $^{12}\text{C}$ , leaving behind the residual DIC pool relatively enriched in  $^{13}\text{C}$  (Whiticar, 1999; Chen et al., 2010; Kim et al., 2011). This interpretation is supported by the cation-adjusted  $\Delta\text{DIC}$  to  $\Delta\text{SO}_4^{2-}$  ratios, which indicate a contribution from deeper zones.

At the Gelendzhik MV, the  $\delta^{13}\text{C}_{\text{DIC}}$  profile exhibits a complex pattern, ranging from  $-11.4\%$  near the sediment-water interface to more depleted values of  $-22.4\%$  at 13.5 cmbsf, followed by a shift toward less depleted values at depth ( $16.1\%$ ; Figure 5). The

pronounced  $\delta^{13}\text{C}_{\text{DIC}}$  depletion at 13.5 cmbsf likely corresponds to an active AOM zone, as such zones typically exhibit strong  $^{13}\text{C}_{\text{DIC}}$  depletion (Whiticar, 1999). The reversal toward less depleted values at depth indicates influence of DIC contribution from deeper sources, consistent with stoichiometric evidence for dominant AOM-SR and high methane concentrations. These observations point to a significant contribution of  $^{13}\text{C}$ -depleted DIC from both AOM activity and upward diffusion from deeper sedimentary layers.

The depth of maximal  $\delta^{13}\text{C}_{\text{DIC}}$  depletion likely corresponds to an active AOM zone (Haese et al., 2003; Chen et al., 2010). To test this interpretation, an end-member mixing model based on chlorinity and  $\delta^{13}\text{C}_{\text{DIC}}$  values was applied. Using chlorinity end members of 631 mM (overlying seawater), 1512 mM (proposed active AOM-SR zone), and 1989 mM (deepest core sample at Gelendzhik), the pore fluid at 13.5 cmbsf is estimated to consist of  $\sim 35\%$  overlying seawater and  $\sim 65\%$  deep fluid. Using this mixing ratio, the expected  $\delta^{13}\text{C}_{\text{DIC}}$  value would be  $-14.5\%$ , whereas the measured value is  $-22.4\%$ . This additional  $-7.9\%$  depletion is therefore attributed to *in situ* AOM activity, providing evidence for an active AOM zone at this depth.

#### 4.3.3 OSR and AOM-SR at hypersaline environments

At the Gelendzhik and Heraklion MVs, OSR and AOM-SR occur under hypersaline conditions. Similar findings have been reported from other Mediterranean MVs, such as Chefreden and

Napoli MVs, where AOM and OSR were observed at salinities up to 153 and 268‰, respectively (Omeregine et al., 2009). In the Tyro and Bannock brines (salinity ~260‰), sulfate-reducing bacteria were likewise active, indicating that extreme salinity does not necessarily inhibit organic matter degradation via sulfate reduction (Henneke et al., 1997). At the Mercator MV, AOM-related microorganisms thrived at salinities approaching halite saturation (Maignien et al., 2013). Beyond the Mediterranean, molecular evidence of AOM has been reported in hypersaline Gulf of Mexico sediments (Lloyd et al., 2006) and in continental hypersaline environments, such as the Salitral Negro lake, where diverse halophilic microbial communities are capable of anaerobic metabolism using various electron acceptors, including sulfate (Solchaga et al., 2022).

## 4.4 Deep-sourced imprint in the DIC pool

### 4.4.1 Isotopic composition of diagenetically added DIC

To distinguish *in situ* produced DIC from deep-sourced DIC, we estimated the isotopic composition of diagenetically added DIC to the pore-water pool using a  $\delta^{13}\text{C}_{\text{DIC}} \times \text{DIC}$  versus DIC plot

following Miller and Tans (2003). The slope represents the isotopic signature of the carbon source undergoing mineralization (Martin et al., 2000; Hu et al., 2010; Coffin et al., 2013; Wu et al., 2016). At the Gelendzhik MV,  $\delta^{13}\text{C}_{\text{added}}$  value was estimated at -53.1‰ (Table 2), indicating a strong contribution from AOM-SR (Coffin et al., 2013). At Milano MV, the  $\delta^{13}\text{C}_{\text{added}}$  was also depleted (-34.1‰), suggesting AOM-SR influence. In contrast, Heraklion and Moscow MVs had less negative values (-28.45‰, and -22.87‰, respectively), consistent with a dominant OSR signal (Figure 8). These results highlight spatial variability in diagenetically carbon sources: AOM-SR dominates at Gelendzhik, OSR at Heraklion and Moscow, while Milano reflects a mixed contribution.

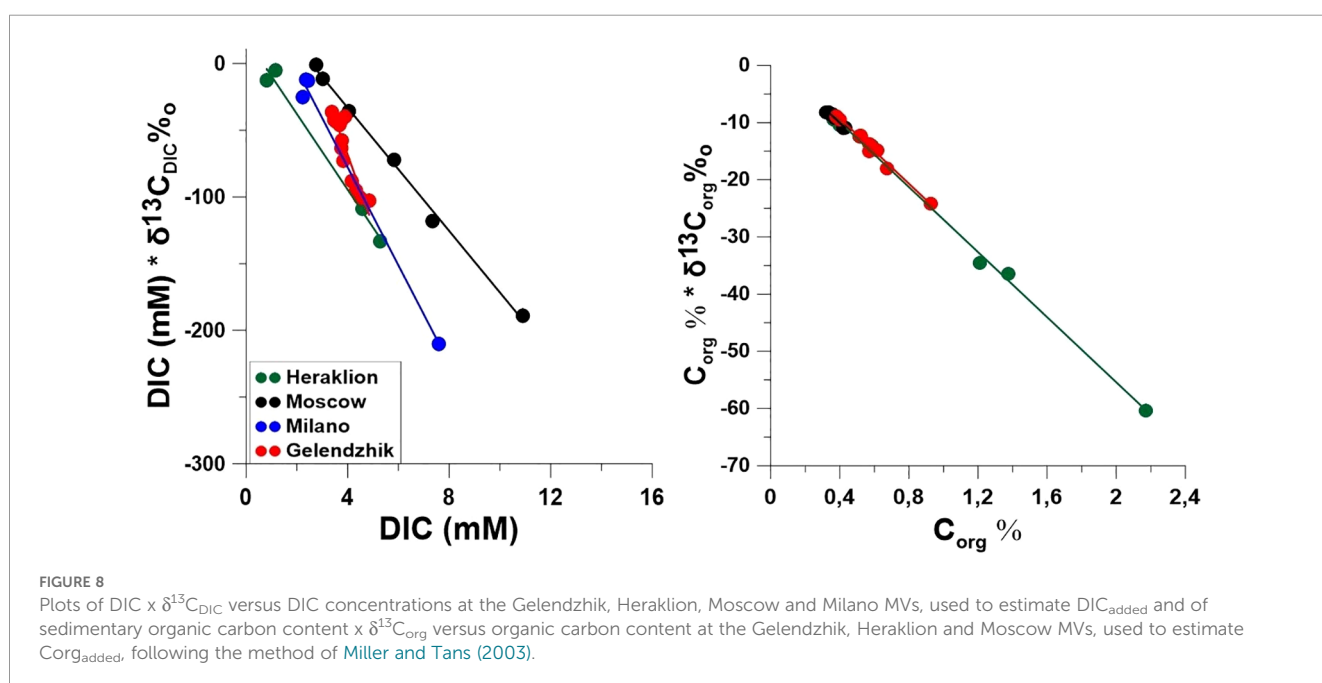
### 4.4.2 Isotopic composition of diagenetically added organic carbon

To assess carbon sources, we examined the sedimentary organic carbon pool. Using the  $\delta^{13}\text{C}_{\text{org}} \times C_{\text{org}}$  versus  $C_{\text{org}}$  plot (Figure 8), we estimated the isotopic signature that organic carbon within the sediments, would exhibit upon remineralization. Unfortunately, data for Milano MV are available. The estimated slopes were -28.8‰, -30.4‰, and -28.0‰ at the Gelendzhik, Heraklion, and Moscow MVs, respectively (Table 2), more depleted than typical Eastern

TABLE 2 Slope and  $R^2$  values for  $\delta^{13}\text{C}$  versus C plots at Gelendzhik, Heraklion, Moscow and Milano MVs.

Site	$\delta^{13}\text{C}_{\text{org}} \times C_{\text{org}}$ vs $C_{\text{org}}$ slope	$\delta^{13}\text{C}_{\text{org}} \times C_{\text{org}}$ vs $C_{\text{org}}$ $R^2$	$\delta^{13}\text{C}_{\text{DIC}} \times \text{DIC}$ vs DIC slope	$\delta^{13}\text{C}_{\text{DIC}} \times \text{DIC}$ vs DIC $R^2$
Gelendzhik	-28.8	0.982	-53.1	0.821
Heraklion	-30.4	0.993	-28.4	0.988
Moscow	-28.0	0.960	-22.8	0.996
Milano			-34.1	0.997

$\delta^{13}\text{C}_{\text{org}} \times C_{\text{org}}$  vs  $C_{\text{org}}$  corresponds to organic carbon plots, while  $\delta^{13}\text{C}_{\text{DIC}} \times \text{DIC}$  vs DIC corresponds to DIC plots.



Mediterranean pelagic sediments, suggesting contributions from methane-derived biomass (Aloisi et al., 2000; Haese et al., 2003). These values do not demonstrate strong spatial variability among the studied MVs.

#### 4.4.3 Does DIC originate from *in situ* organic matter mineralization?

By comparing the  $\delta^{13}\text{C}$  signature of diagenetically added DIC and sedimentary organic carbon, we assess whether DIC originates from *in situ* organic matter mineralization or from deeper sources. At Heraklion, the DIC added (-28.4‰) is close to  $\text{C}_{\text{org added}}$  (-30.4‰), suggesting that DIC is mainly produced via local OSR. At Moscow, the DIC added (-22.8‰) is enriched relative to sedimentary organic carbon pool (-28.0‰), suggesting a significant component of deep-sourced,  $^{13}\text{C}$ -enriched DIC from upward diffusion from methanogenic zones. At Gelendzhik, the large offset between DIC added (-53.1‰) and sedimentary organic carbon (-28.8‰) indicates a dominant AOM signal and *in situ* methane cycling.

These  $\delta^{13}\text{C}$  isotopic offsets at Gelendzhik and Moscow MVs highlight distinct carbon sources for pore fluids and sedimentary organic matter, indicating fluid migration and degassing from deeper methanogenic strata. Porewater geochemistry at these sites is influenced both by ongoing shallow diagenetic processes and upward transport of deep-sourced fluids and gases.

## 5 Conclusions

This study demonstrates that pore water geochemistry in the OMVF can be classified into two distinct geochemical groups with characteristic chemical depth profiles. The first group, represented by Gelendzhik and Heraklion MVs, is dominated by hypersaline fluids enriched in sodium, chloride, sulfate, and ammonium, reflecting deep, highly saline fluids derived below Messinian evaporites. The second group, comprising Moscow and Milano mud volcanoes, shows near-seawater salinity and limited influence from deep brines. These geochemical groups reflect underlying differences in fluid sources and migration pathways, providing a framework to understand solute and methane dynamics across the OMVF.

High-resolution pore water data from the upper sediment layers reveal pronounced spatial heterogeneity in major ions, ammonium, methane, and  $\delta^{13}\text{C}_{\text{DIC}}$  concentrations across the studied MVs. In the hypersaline group, deep-sourced fluids are further modified by diagenetic processes, including silicate interaction or dissolution of K-rich minerals at Gelendzhik and smectite-illite transformation at Heraklion. Spatial variability in ammonium concentrations and in ammonium to DIC ratios between Gelendzhik and Heraklion also suggests variations in fluid pathways and diagenetic overprints. In contrast, the surficial pore fluids at Moscow and Milano MVs show no clear evidence of deep-brine influx and reflect predominantly seawater-derived concentrations.

Sulfate-consuming processes and carbon cycling also vary among the studied MVs. Methane concentrations and  $\delta^{13}\text{C}_{\text{DIC}}$

values indicates degassing of deep sediments. At Gelendzhik MV, AOM-SR dominates within a DIC-depleted system. At Moscow MV, *in situ* OSR occurs alongside deep-sourced DIC input from methanogenic zones. These results provide geochemical evidence for OSR and AOM occur under extreme hypersaline environments at the Gelendzhik and Heraklion MVs. The  $\delta^{13}\text{C}$  signatures of diagenetically added DIC and sedimentary organic carbon demonstrate that DIC originates not only from *in situ* organic matter mineralization but also from deeper sources. Overall, the data highlight the highly heterogeneous and dynamic nature of the OMVF mud volcanoes, which act not only as conduits for complex fluid and gas migration but also as active sites where deep and early diagenesis intersect.

Despite shallow sampling depths across all sites, the spatial geochemical heterogeneity observed reflects the combined imprint of deep-sourced fluid and gas influx through multiple diagenetic processes that occurred prior to fluid ascent well below the seafloor. These findings highlight the complexity of fluid pathways in tectonically active mud-volcano provinces, underscore the importance of multi-parameter, high-resolution studies, and demonstrate how multiple processes can generate substantial geochemical heterogeneity at very small spatial scales.

## Data availability statement

The original contributions presented in the study are included in the article/Supplementary Material. Further inquiries can be directed to the corresponding author.

## Author contributions

ER: Conceptualization, Data curation, Investigation, Methodology, Validation, Writing – original draft, Writing – review & editing. PM: Conceptualization, Supervision, Writing – review & editing. AP: Supervision, Writing – review & editing. IH: Data curation, Methodology, Writing – review & editing. HK: Writing – review & editing. SI: Methodology, Writing – review & editing. GR: Resources, Writing – review & editing.

## Funding

The author(s) declared that financial support was received for this work and/or its publication. The present study was funded by the Greek General Secretariat of Research and Technology under the framework of the Programming Agreements between Research Centers and GSRT/IKY/SIEMENS 2014–2016.

## Acknowledgments

The authors would like to thank the crew of *R/V Aegaeo* and the scientific party for the excellent support during the LEVECO cruise. We are grateful to Yale Analytical and Technical laboratories for the

$\delta^{13}\text{C}_{\text{DIC}}$  analysis. We would like to thank Chara Kyriakidou for modifying the map used in this paper. The present work was funded by the Greek General Secretariat of Research and Technology under the framework of the Programming Agreements between Research Centers and GSRT/IKY/SIEMENS 2014–2016.

## Conflict of interest

The authors declared that this work was conducted in the absence of any commercial or financial relationships that could be construed as a potential conflict of interest.

## Generative AI statement

The author(s) declared that generative AI was not used in the creation of this manuscript.

Any alternative text (alt text) provided alongside figures in this article has been generated by Frontiers with the support of artificial

intelligence and reasonable efforts have been made to ensure accuracy, including review by the authors wherever possible. If you identify any issues, please contact us.

## Publisher's note

All claims expressed in this article are solely those of the authors and do not necessarily represent those of their affiliated organizations, or those of the publisher, the editors and the reviewers. Any product that may be evaluated in this article, or claim that may be made by its manufacturer, is not guaranteed or endorsed by the publisher.

## Supplementary material

The Supplementary Material for this article can be found online at: <https://www.frontiersin.org/articles/10.3389/fmars.2025.1728781/full#supplementary-material>

## References

- Aloisi, G., Drews, M., Wallmann, K., and Bohrmann, G. (2004). Fluid expulsion from the Dvurechenskii mud volcano (Black Sea). Part I. Fluid sources and relevance to Li, B C.OMMAS.R.X.X.X, I and dissolved inorganic nitrogen cycles. *Earth Planet. Sci. Lett.* 225, 347–363. doi: 10.1016/j.epsl.2004.07.006
- Aloisi, G., Pierre, C., Rouchy, J. M., Foucher, J. P., and Woodside, J. (2000). Methane-related authigenic carbonates of Eastern Mediterranean Sea mud volcanoes and their possible relation to gas hydrate destabilisation. *Earth Planet. Sci. Lett.* 184, 321–338. doi: 10.1016/S0012-821X(00)00322-8
- Behrendt, N., Menapace, W., Bohrmann, G., Zabel, M., and Kopf, A. J. (2023). Pore water signatures and gas hydrates occurrence in and around the Olimpi mud volcano field, south of Crete. *Mar. Pet. Geol.* 156, 106429. doi: 10.1016/j.marpetgeo.2023.106429
- Boetius, A., Ravensschlag, K., Schubert, C. J., Rickert, D., Widdel, F., Gieseke, A., et al. (2000). A marine microbial consortium apparently mediating anaerobic oxidation of methane. *Lett. to Nat.* 407, 623–626. doi: 10.1038/35036572
- Bohrmann, G., Ivanov, M., Foucher, J. P., Spiess, V., Bialas, J., Greinert, J., et al. (2003). Mud volcanoes and gas hydrates in the Black Sea: New data from Dvurechenskii and Odessa mud volcanoes. *Geo-Marine. Lett.* 23, 239–249. doi: 10.1007/s00367-003-0157-7
- Borowski, W. S., Paull, C. K., and Ussler, W. III (1996). Marine pore-water sulfate profiles indicate in situ methane flux from underlying gas hydrate. *Geology* 24, 655–658. doi: 10.1130/0091-7613(1996)024<0655:MPWSP>2.3.CO;2
- Böttcher, M. E., Brumsack, H.-J., and de Lange, G. J. (1998). Sulfate reduction and related stable isotope ( $^{34}\text{S}$ ,  $^{18}\text{O}$ ) variations in interstitial waters from the eastern Mediterranean. *Proc. Ocean. Drill. Program. Sci. Results.* 160, 365–373.
- Bryant, C. L., Henley, S. F., Murray, C., Ganeshram, R. S., and Shanks, R. (2013). Storage and hydrolysis of seawater samples for inorganic carbon isotope analysis. *Radiocarbon* 55, 401–409. doi: 10.1017/s0033822200057520
- Camerlenghi, A., Cita, M. B., Della Vedova, B., Fusi, N., Mirabile, L., and Pellis, G. (1995). Geophysical evidence of mud diapirism on the Mediterranean ridge accretionary complex. *Mar. Geophys. Res.* 17, 115–141. doi: 10.1007/BF01203423
- Camerlenghi, A., Cita, M. B., Hieke, W., and Ricchiuto, T. (1992). Geological evidence for mud diapirism on the Mediterranean Ridge accretionary complex. *Earth Planet. Sci. Lett.* 109, 493–504. doi: 10.1016/0012-821X(92)90109-9
- Chen, T., Strauss, H., Fang, Y., Lin, Z., Sun, X., Liu, J., et al. (2022). Sulfur and oxygen isotope records of sulfate-driven anaerobic oxidation of methane in diffusion-dominated marine sediments. *Front. Earth Sci.* 10. doi: 10.3389/feart.2022.862333
- Chen, Y., Ussler, W., Hafliadason, H., Lepland, A., Rise, L., Hovland, M., et al. (2010). Sources of methane inferred from pore-water  $\delta^{13}\text{C}$  of dissolved inorganic carbon in Pockmark G11, offshore Mid-Norway. *Chem. Geol.* 275, 127–138. doi: 10.1016/j.chemgeo.2010.04.013
- Cita, M. B., Erba, E., Lucchi, R., Pott, M., van der Meer, R., and Nieto, L. (1996). Stratigraphy and sedimentation in the Mediterranean Ridge diapiric belt. *Mar. Geol.* 132, 131–150. doi: 10.1016/0025-3227(96)00157-0
- Cline, J. D. (1969). Spectrophotometric determination of hydrogen sulfide in natural waters. *Limnol. Oceanogr.* 14, 454–458. doi: 10.4319/lo.1969.14.3.0454
- Coffin, R. B., Smith, J. P., Plummer, R. E., Yoza, B., Larsen, R. K., Millholland, L. C., et al. (2013). Spatial variation in shallow sediment methane sources and cycling on the Alaskan Beaufort Sea Shelf/Slope. *Mar. Pet. Geol.* 45, 186–197. doi: 10.1016/j.marpetgeo.2013.05.002
- Dählmann, A., and de Lange, G. (2003). Fluid–sediment interactions at Eastern Mediterranean mud volcanoes: a stable isotope study from ODP Leg 160. *Earth Planet. Sci. Lett.* 212, 377–391. doi: 10.1016/S0012-821X(03)00227-9
- Deyhle, A., and Kopf, A. (2001). Deep fluids and ancient pore waters at the backstop: Stable isotope systematics (B, C, O) of mud-volcano deposits on the Mediterranean Ridge accretionary wedge. *Geology* 29, 1031–1034. doi: 10.1130/0091-7613(2001)029<1031:DFAAPW>2.0.CO;2
- Dijkstra, N., Kraal, P., Kuypers, M. M. M., Schnetger, B., and Slomp, C. P. (2014). Are iron-phosphate minerals a sink for phosphorus in anoxic black sea sediments? *PLoS One* 9, 1–12. doi: 10.1371/journal.pone.0101139
- Dimitrov, L. (2002). Mud volcanoes - the most important pathway for degassing deeply buried sediments. *Earth-Sci. Rev.* 59, 49–76. doi: 10.1016/S0012-8252(02)00069-7
- Doll, M., Römer, M., Pape, T., Kölling, M., Kaul, N., dos Santos Ferreira, C., et al. (2023). Recent and episodic activity of decoupled mud/fluid discharge at Sartori mud volcano in the Calabrian Arc, Mediterranean Sea. *Front. Earth Sci.* 11. doi: 10.3389/feart.2023.1181380
- Egger, M., Jilbert, T., Behrends, T., Rivard, C., and Slomp, C. P. (2015). Vivianite is a major sink for phosphorus in methanogenic coastal surface sediments. *Geochim. Cosmochim. Acta* 169, 217–235. doi: 10.1016/j.gca.2015.09.012
- Egger, M., Lenstra, W., Jong, D., Meysman, F. J. R., Sapart, C. J., van der Veen, C., et al. (2016). Rapid sediment accumulation results in high methane effluxes from coastal sediments. *PLoS One* 11, 1–22. doi: 10.1371/journal.pone.0161609
- Fontugne, M. R., and Calvert, S. E. (1992). Late pleistocene variability of the carbon isotopic composition of organic matter in the eastern Mediterranean: monitor of changes in carbon sources and atmospheric CO<sub>2</sub> concentrations. *Palaeogeogr. Palaeoclimatol.* 7, 1–20. doi: 10.1029/91PA02674
- Haese, R. R., Hensen, C., and De Lange, G. J. (2006). Pore water geochemistry of eastern Mediterranean mud volcanoes: Implications for fluid transport and fluid origin. *Mar. Geol.* 225, 191–208. doi: 10.1016/j.margeo.2005.09.001
- Haese, R. R., Meile, C., Van Cappellen, P., and De Lange, G. J. (2003). Carbon geochemistry of cold seeps: Methane fluxes and transformation in sediments from Kazan mud volcano, eastern Mediterranean Sea. *Earth Planet. Sci. Lett.* 212, 361–375. doi: 10.1016/S0012-821X(03)00226-7
- Hall and Aller (1992). Rapid, small-volume, flow injection marine and freshwaters analysis for  $\Sigma\text{CO}_2$  and  $\text{NH}_4^+$  in marine and freshwaters. *Limnol. Oceanogr. Methods* 37, 1113–1119. doi: 10.1109/TMAG.2009.2017530

- Henneke, E., Luther, G. W., De Lange, G. J., and Hoefs, J. (1997). Sulphur speciation in anoxic hypersaline sediments from the eastern Mediterranean Sea. *Geochim. Cosmochim. Acta* 61, 307–321. doi: 10.1016/S0016-7037(96)00355-9
- Hensen, C., Nuzzo, M., Hornibrook, E., Pinheiro, L. M., Bock, B., Magalhães, V. H., et al. (2007). Sources of mud volcano fluids in the Gulf of Cadiz-indications for hydrothermal imprint. *Geochim. Cosmochim. Acta* 71, 1232–1248. doi: 10.1016/j.gca.2006.11.022
- Hensen, C., Pfeifer, Z. M., Schwenk, T., Kasten, S., Riedinger, N., Schulz, H. D., et al. (2003). Control of sulfate pore-water profiles by sedimentary events and the significance of anaerobic oxidation of methane for the burial of sulfur in marine sediments. *Geochim. Cosmochim. Acta* 67, 2631–2647. doi: 10.1016/S0016-7037(00)00199-6
- Hinrichs, K. U., Hayes, J. M., Sylva, S. P., Brewert, P. G., and DeLong, E. F. (1999). Methane-consuming archaeobacteria in marine sediments. *Nature* 398, 802–805. doi: 10.1038/19751
- Hu, X., Cai, W.-J., Wang, Y., Luo, S., and Guo, X. (2010). Pore-water geochemistry of two contrasting brine-charged seep sites in the northern Gulf of Mexico continental slope. *Mar. Chem.* 118, 99–107. doi: 10.1016/j.marchem.2009.11.006
- Huguen, C., Mascle, J., Chaumillon, E., Kopf, A., Woodside, J., and Zitter, T. (2004). Structural setting and tectonic control of mud volcanoes from the Central Mediterranean Ridge (Eastern Mediterranean). *Mar. Geol.* 209, 245–263. doi: 10.1016/j.margeo.2004.05.002
- Huguen, C., Mascle, J., Woodside, J., Zitter, T., and Foucher, J. P. (2005). Mud volcanoes and mud domes of the Central Mediterranean Ridge: Near-bottom and *in situ* observations. *Deep. Res. Part I. Oceanogr. Res. Pap.* 52, 1911–1931. doi: 10.1016/j.dsr.2005.05.006
- Ijiri, A., Setoguchi, R., Mitsutome, Y., Toki, T., Murayama, M., Hagino, K., et al. (2023). Origins of sediments and fluids in submarine mud volcanoes off Tanegashima Island, northern Ryukyu Trench, Japan. *Front. Earth Sci.* 11. doi: 10.3389/feart.2023.1206810
- Jørgensen, B. B., Beulig, F., Egger, M., Petro, C., Scholze, C., and Roy, H. (2019a). Organoclastic sulfate reduction in the sulfate-methane transition of marine sediments. *Geochim. Cosmochim. Acta* 254, 231–245. doi: 10.1016/j.gca.2019.03.016
- Jørgensen, B. B., Findlay, A. J., and Pellerin, A. (2019b). The biogeochemical sulfur cycle of marine sediments. *Front. Microbiol.* 10. doi: 10.3389/fmicb.2019.00849
- Jørgensen, B. B., and Kasten, S. (2006). Sulfur cycling and methane oxidation. *Mar. Geochim.* 271–309. doi: 10.1007/3-540-32144-6\_8
- Kastner, M., Claypool, G., and Robertson, G. (2008). Geochemical constraints on the origin of the pore fluids and gas hydrate distribution at Atwater Valley and Keathley Canyon, northern Gulf of Mexico. *Mar. Pet. Geol.* 25, 860–872. doi: 10.1016/j.marpetgeo.2008.01.022
- Kastner, M., Elderfield, H., and Martin, J. B. (1991). Fluids in Convergent Margins: What do We Know about their Composition, Origin, Role in Diagenesis and Importance for Oceanic Chemical Fluxes? *Philos. Trans. R. Soc. B. Biol. Sci.* 12, 243–259. doi: 10.1098/rsta.1991.0045
- Kim, J. H., Park, M. H., Chun, J. H., and Lee, J. Y. (2011). Molecular and isotopic signatures in sediments and gas hydrate of the central/southwestern Ulleung Basin: High alkalinity escape fuelled by biogenically sourced methane. *Geo-Marine. Lett.* 31, 37–49. doi: 10.1007/s00367-010-0214-y
- Kopf, A. J. (2002). Significance of mud volcanism. *Rev. Geophys.* 40, 1–52. doi: 10.1029/2000RG000093
- Kopf, A., Robertson, A. H. F., and Volkman, N. (2000). Origin of mud breccia from the Mediterranean Ridge accretionary complex based on evidence of the maturity of organic matter and related petrographic and regional tectonic evidence. *Mar. Geol.* 166, 65–82. doi: 10.1016/S0025-3227(00)00009-8
- Koroleff, F. (1970). Direct determination of ammonia in natural waters as indophenol blue. *Inf. Tech. Methods Seawater. Anal.*, 19–22.
- Lee, D. H., Kim, J. H., Lee, Y. M., Kim, J. H., Jin, Y. K., Paull, C., et al. (2021). Geochemical and microbial signatures of siboglinid tubeworm habitats at an active mud volcano in the Canadian Beaufort Sea. *Front. Mar. Sci.* 8. doi: 10.3389/fmars.2021.656171
- Li, N., Huang, H., and Chen, D. (2014). Fluid sources and chemical processes inferred from geochemistry of pore fluids and sediments of mud volcanoes in the southern margin of the Junggar Basin, Xinjiang, northwestern China. *Appl. Geochem.* 46, 1–9. doi: 10.1016/j.apgeochem.2014.04.007
- Lichtschat, A., Felden, J., Wenzhöfer, F., Schubotz, F., Ertefai, T. F., Boetius, A., et al. (2010). Methane and sulfide fluxes in permanent anoxia: *In situ* studies at the Dvurechenskii mud volcano (Sorokin Trough, Black Sea). *Geochim. Cosmochim. Acta* 74, 5002–5018. doi: 10.1016/j.gca.2010.05.031
- Limonov, A. F., Woodside, J. M., Cita, M. B., and Ivanov, M. K. (1996). The Mediterranean Ridge and related mud diapirism: a background. *Mar. Geol.* 132, 7–19. doi: 10.1016/0025-3227(96)00150-8
- Lloyd, K. G., Lapham, L., and Teske, A. (2006). An anaerobic methane-oxidizing community of ANME-1b archaea in hypersaline gulf of Mexico sediments. *Appl. Environ. Microbiol.* 72, 7218–7230. doi: 10.1128/AEM.00886-06
- López-Rodríguez, C., De Lange, G. J., Comas, M., Martínez-Ruiz, F., Nieto, F., Sapart, C. J., et al. (2019). Recent, deep-sourced methane/mud discharge at the most active mud volcano in the western Mediterranean. *Mar. Geol.* 408, 1–17. doi: 10.1016/j.margeo.2018.11.013
- Maignien, L., Parkes, R. J., Cragg, B., Niemann, H., Knittel, K., Coulon, S., et al. (2013). Anaerobic oxidation of methane in hypersaline cold seep sediments. *FEMS Microbiol. Ecol.* 83, 214–231. doi: 10.1111/j.1574-6941.2012.01466.x
- Martin, J. B., Kastner, M., Henry, P., Le Pichon, X., and Lallement, S. (1996). Chemical and isotopic evidence for sources of fluids in a mud volcano field seaward of the Barbados accretionary wedge. *J. Geophys. Res. Solid. Earth* 101, 20325–20345. doi: 10.1029/96JB00140
- Martin, W. R. R., McNichol, A. P. P., and McCorkle, D. C. C. (2000). The radiocarbon age of calcite dissolving at the sea floor: Estimates from pore water data. *Geochim. Cosmochim. Acta* 64, 1391–1404. doi: 10.1016/S0016-7037(99)00424-X
- Masuzawa, T., Handa, N., Kitagawa, H., and Kusakabe, M. (1992). Sulfate reduction using methane in sediments beneath a bathyal “cold seep” giant clam community off Hatsushima Island, Sagami Bay, Japan. *Earth Planet. Sci. Lett.* 110, 39–50. doi: 10.1016/0012-821X(92)90037-V
- Mazzini, A., and Etiope, G. (2017). Mud volcanism: An updated review. *Earth-Sci. Rev.* 168, 81–112. doi: 10.1016/j.earscirev.2017.03.001
- Milkov, A. V. (2000). Worldwide distribution of submarine mud volcanoes and associated gas hydrates. *Mar. Geol.* 167, 29–42. doi: 10.1016/S0025-3227(00)00022-0
- Miller, J. B., and Tans, P. P. (2003). Calculating isotopic fractionation from atmospheric measurements at various scales. *Tellus. Ser. B. Chem. Phys. Meteorol.* 55, 207–214. doi: 10.1034/j.1600-0889.2003.00020.x
- Moore, J. C., and Vrolijk, P. (1992). Fluids in accretionary prisms. *Rev. Geophys.* 30, 113–135. doi: 10.1029/92RG00201
- Mullin, J. B., and Riley, J. P. (1955). The colorimetric determination of silicate with special reference to sea and natural waters. *Anal. Chim. Acta* 12, 162–176. doi: 10.1016/S0003-2670(00)87825-3
- Murphy, J., and Riley, J. P. (1962). A modified single solution method for the determination of phosphate in natural waters. *Anal. Chim. Acta* 27, 31–36. doi: 10.1016/S0003-2670(00)88444-5
- Niewöhner, C., Hensen, C., Kasten, S., Zabel, M., and Schulz, H. (1998). Deep sulfate reduction completely mediated by anaerobic methane oxidation in sediments of the upwelling area off Namibia. *Geochim. Cosmochim. Acta* 62, 455–464. doi: 10.1016/S0016-7037(98)00055-6
- Omorgie, E. O., Niemann, H., Mastalerz, V., de Lange, G. J., Stadnitskaia, A., Mascle, J., et al. (2009). Microbial methane oxidation and sulfate reduction at cold seeps of the deep Eastern Mediterranean Sea. *Mar. Geol.* 261, 114–127. doi: 10.1016/J.MARGE.2009.02.001
- Panagiotopoulos, I. P., Paraschos, F., Rousakis, G., Hatzianestis, I., Parinos, C., Morfis, I., et al. (2020). Assessment of the eruptive activity and identification of the mud breccia's source in the Olimpi mud volcano field, Eastern Mediterranean. *Deep. Res. Part II. Top. Stud. Oceanogr.* 171. doi: 10.1016/j.dsr2.2019.104701
- Saffer, D. M., and Tobin, H. J. (2011). Hydrogeology and mechanics of subduction zone forearcs: fluid flow and pore pressure. *Annu. Rev. Earth Planet. Sci.* 39, 157–186. doi: 10.1146/annurev-earth-040610-133408
- Scholz, F., Hensen, C., Schmidt, M., and Geersen, J. (2013). Submarine weathering of silicate minerals and the extent of pore water freshening at active continental margins. *Geochim. Cosmochim. Acta* 100, 200–216. doi: 10.1016/j.gca.2012.09.043
- Snyder, G. T., Hiruta, A., Matsumoto, R., Dickens, G. R., Tomaru, H., Takeuchi, R., et al. (2007). Pore water profiles and authigenic mineralization in shallow marine sediments above the methane-charged system on Umitaka Spur, Japan Sea. *Deep. Res. Part II. Top. Stud. Oceanogr.* 54, 1216–1239. doi: 10.1016/j.dsr2.2007.04.001
- Solchaga, J. I., Busalmen, J. P., and Nercessian, D. (2022). Unraveling anaerobic metabolisms in a hypersaline sediment. *Front. Microbiol.* 13. doi: 10.3389/fmicb.2022.811432
- Thompson, T., Johnston, W. R., and Wirth, H. E. (1931). The Sulfate-Chlorinity Ratio in Ocean Waters. Available online at: <https://academic.oup.com/icesjms/article/6/2/246/600439> (Accessed November 25, 2025).
- Torres, M. E., Hong, W. L., Solomon, E. A., Milliken, K., Kim, J. H., Sample, J. C., et al. (2020). Silicate weathering in anoxic marine sediment as a requirement for authigenic carbonate burial. *Earth-Sci. Rev.* 200, 102960. doi: 10.1016/j.earscirev.2019.102960
- Tsabarlis, C., Patiris, D. L. L., Pappa, F. K. K., Alexakis, S., and Michalopoulos, P. (2020). Preliminary investigation of olimpi field, Mediterranean Sea, using *in-situ* and laboratory radio-tracing methods. *Deep. Res. Part II. Top. Stud. Oceanogr.* 171, 104689. doi: 10.1016/j.dsr2.2019.104689
- Vanneste, H., Kelly-Gerreyn, B. A., Connelly, D. P., James, R. H., Haeckel, M., Fisher, R. E., et al. (2011). Spatial variation in fluid flow and geochemical fluxes across the sediment-seawater interface at the Carlos Ribeiro mud volcano (Gulf of Cadiz). *Geochim. Cosmochim. Acta* 75, 1124–1144. doi: 10.1016/j.gca.2010.11.017
- Wallmann, K., Aloisi, G., Haeckel, M., Tishchenko, P., Pavlova, G., Greinert, J., et al. (2008). Silicate weathering in anoxic marine sediments. *Geochim. Cosmochim. Acta* 72, 2895–2918. doi: 10.1016/j.gca.2008.03.026
- Whiticar, M. (1999). Carbon and hydrogen isotope systematics of bacterial formation of methane. *Chem. Geol.* 161, 291. doi: 10.1016/S0009-2541(99)00092-3
- Wu, Z. J., Zhou, H. Y., Ren, D. Z., Gao, H., and Li, J. T. (2016). Quantifying the sources of dissolved inorganic carbon within the sulfate-methane transition zone in nearshore sediments of Qi'ao Island, Pearl River Estuary, Southern China. *Sci. China Earth Sci.* 59, 1959–1970. doi: 10.1007/s11430-016-0057-0
- Zhang, Z. (2020). Rapid shifts in chemical and isotopic compositions of sediment pore waters in the amami sankaku basin in response to initial arc rifting in the mid-oligocene. *Geochim. Geophys. Geosyst.* 21, e2019GC008845. doi: 10.1029/2019GC008845